Stability of *Hoogsteen*-Type Triplexes – Electrostatic Attraction between Duplex Backbone and Triplex-Forming Oligonucleotide (TFO) Using an Intercalating Conjugate

by **Daniel Globisch**[a]), **Niels Bomholt**[a]), **Vyacheslav V. Filichev**[b]), and **Erik B. Pedersen***[a])

[a]) Nucleic Acid Center, Department of Physics and Chemistry, University of Southern Denmark, Campusvej 55, DK-5230 Odense M
(phone: +4565502555; fax: +4566158780; e-mail: ebp@ifk.sdu.dk)
[b]) Institute of Fundamental Sciences, Massey University, Private Bag 11-222, Palmerston North, New Zealand

Syntheses are described for two novel twisted intercalating nucleic acid (TINA) monomers where the intercalator comprises a benzene ring linked to a naphthalimide moiety *via* an ethynediyl bridge. The intercalators **Y** and **Z** have a 2-(dimethylamino)ethyl and a methyl residue on the naphthalimide moiety, respectively. When used as triplex-forming oligonucleotides (TFOs), the novel naphthalimide TINAs show extraordinary high thermal stability in *Hoogsteen*-type triplexes and duplexes with high discrimination of mismatch strands. DNA Strands containing the intercalator **Y** show higher thermal triplex stability than DNA strands containing the intercalator **Z**. This observation can be explained by the ionic interaction of the protonated dimethylamino group under physiological conditions, targeting the negatively charged phosphate backbone of the duplex. This interaction leads to an extra binding mode between the TFO and the duplex, in agreement with molecular-modeling studies. We believe that this is the first example of an intercalator linking the TFO to the phosphate backbone of the duplex by an ionic interaction, which is a promising tool to achieve a higher triplex stability.

Introduction. – Triplex-forming oligonucleotides (TFOs) are of great interest due to their application in antigene strategy. The gene expression of malfunctioned genes is blocked in this technology before the transcription step. Contrary to antisense agents, there are no antigene agents in clinical trials. The advantage of the antigene strategy should be the inhibition of gene expression at the first step, hence targeting of only two copies instead of up to thousands of mRNA copies in the antisense approach. For the success of antigene strategy, it is necessary to enhance stabilization of triplexes by novel TFOs, due to low stability of natural TFOs, and the limitation of sufficiently long homopurine/homopyrimidine stretches in the target DNA for triplex formation [1]. These facts and the quadruplex formation of G-rich strands are the major drawback for the success of this strategy [2]. To increase the stability of triplexes, an enormous number of chemically modified oligodeoxynucleotides (ONs) have been developed for their use as TFOs. Improved stabilization can be achieved by either modifying the nucleobase [3], the sugar part [4], or the phosphate backbone [5]. In some of these approaches, enhanced triplex stabilities are possible by reducing the unfavorable charge repulsion between the three negatively charged DNA strands under physiological conditions. Exchange of negatively charged O-atoms in the phosphate backbone by uncharged heteroatoms led to an increased stabilization of the triplex. In another

method, the repulsion was reduced by an amino side chain, which is protonated under physiological conditions, forming ionic interactions with the phosphate backbone of the TFO itself [3c,d][4a,e][5c].

Another method for stabilization of triplexes is the use of intercalating systems, in which an aromatic system stabilizes the triplex by $\pi-\pi$ interaction with the adjacent nucleobases of the target duplex without disrupting the H-bonds. Pyrene is often used as an aromatic system for intercalation due to its large π-surface and its fluorescence properties [6][7]. An intercalating system, called twisted intercalating nucleic acid (TINA), is named due to a benzene moiety and a large aromatic system, which are supposed to twist around the C≡C bond for better intercalating properties [6a,b]. Every part of this intercalator is able to stabilize the triplex by $\pi-\pi$ interactions. The benzene moiety is assumed to stabilize the nucleobases in the TFO, while the pyrene moiety intercalates with the nucleobases of the duplex. *Froehler et al.* described that a C≡C bond can also enhance the triplex stability [8]. The intercalator is inserted as a bulge without an opposite base.

Pyrene was found to give the best intercalating system **X** compared to other aromatic systems like naphthalene **W**, 1,1′-biphenyl, and various 9-substituted acridines, which showed similar properties as pyrene but with a lower stabilization of the triplexes [6a,b][9] (*Fig. 1*). TFOs containing pyrene-TINA showed triplex stabilities with high discrimination to mismatched *Hoogsteen* binding to duplexes. Another useful effect of these TFOs was destabilization of antiparallel *Watson–Crick* duplexes which may reduce the risk of unwanted side effects when TINA-TFOs eventually are used as drugs. The most important advantage of TINAs has been described recently. It was demonstrated that the intercalator is interfering with quadruplex formation of G-rich oligonucleotides at physiological potassium concentrations releasing the oligonucleotide for antiparallel triplex formation [2b]. This means a double effect of TINA: *i.e.*, destabilization of the quadruplexes and increasing the triplex stability of G-rich TFOs.

In this study, an intercalating system **Y** with an amino side chain attached to the aromatic system was prepared. Under physiological conditions, the positively charged amine forms an ionic interaction to the negatively charged phosphate backbone of the duplex, resulting in an additional binding mode to stabilize the triplex. This intercalator showed an enhanced triplex stability compared to the similar intercalating system without the ionic interaction **Z**. Molecular modeling is used to visualize that the enhanced triplex stability is due to a combination of stacking with the intercalator, and the ionic interaction between the duplex backbone and the amino group in the side chain of the intercalator.

Results and Discussion. – *Synthesis.* The synthesis of both monomers for standard phosphoramidite chemistry started with the condensation of 4-bromonaphthalene-1,8-dicarboxylic anhydride (**1**) with *N*,*N*-dimethylethane-1,2-diamine in EtOH or $MeNH_2$ in EtOH (33% *v*/*v*), to afford 4-bromo-*N*-[2-(dimethylamino)ethyl]-1,8-naphthalimide (**2a**) and 4-bromo-*N*-methyl-1,8-naphthalimide (**2b**) in 74 and 89% yield, respectively [10][11]. The precursor (2*R*)-3-[(4-ethynylbenzyl)oxy]propane-1,2-diol (**3**) [6a][9] and the appropriate naphthalimides **2** were coupled under *Sonogashira* conditions [12] to achieve the *N*-[2-(dimethylamino)ethyl]naphthalimide derivative **4a** and the *N*-methylnaphthalimide derivative **4b** in 78 and 31% yield, respectively (*Scheme 1*).

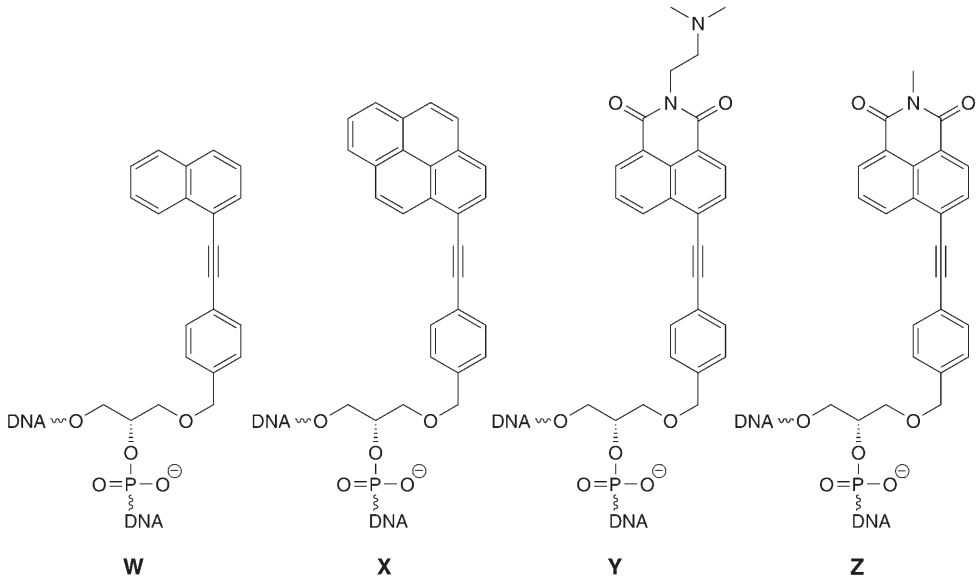

Fig. 1. *The intercalators* **Y** *and* **Z**, *and the reference intercalators* **W** *and* **X**

Scheme 1. *Synthesis of Phosphoramidite Precursors*

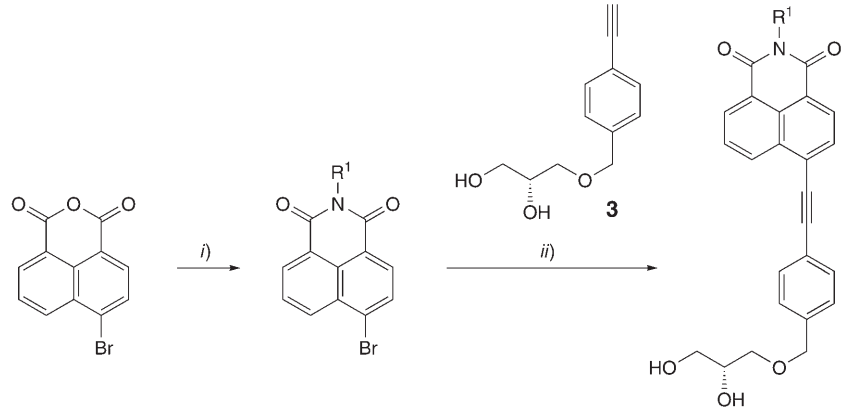

i) R^1NH_2, EtOH, reflux, 3.5–15 h; **2a**: 74%, **2b**: 89%. *ii*) $Pd(PPh_3)_4$, CuI, Et_3N, DMF, 20°, 20–45 h; **4a**: 78%, **4b**: 31%.

The synthesis of the phosphoramidite **7a** was achieved in 38% yield by subsequent DMT-protection of the primary alcohol of **4a** to give **6a**, which was phosphitylated with

2-cyanoethyl *N*,*N*,*N*′,*N*′-(tetraisopropyl)phosphordiamidite in anhydrous CH_2Cl_2 using diisopropylammonium tetrazolide as an activator (*Scheme 2*). When the same strategy was applied for the synthesis of the amidite **7b**, only low yields were obtained in the synthesis of the DMT-protected compound **6b**, although the protection reaction of **4b** was attempted with a variety of methods. Instead, DMT-protection of precursor **3**, followed by *Sonogashira* coupling, considerably improved the yield of the protected compound **6b**. Treatment of **3** with DMTCl in pyridine afforded (*S*)-1-[bis(4-methoxyphenyl)(phenyl)methoxy]-3-[(4-ethynylbenzyl)oxy]propan-2-ol (**5**) in 73% yield. Subsequent *Sonogashira* coupling with naphthalimide **2b** afforded **6b** in 65% yield. The phosphitylated monomer **7b** was then synthesized in 89% yield. Incorporation of both monomers **7a** and **7b** in several DNA sequences was achieved by standard automated DNA syntheses. The synthesized oligonucleotides and their mass-spectrometric analysis are listed in *Table 1*.

Thermal Stability Studies. The thermal stability (melting temperature/T_m,°) of triplexes and different types of duplexes with the synthesized oligonucleotides containing the novel intercalators **Y** and **Z** was assessed by thermal denaturation experiments. The melting temperatures (T_m) are listed in *Tables 2–4*. All oligonucleo-

Scheme 2. *Synthesis of Intercalator* **Y** *and* **Z**

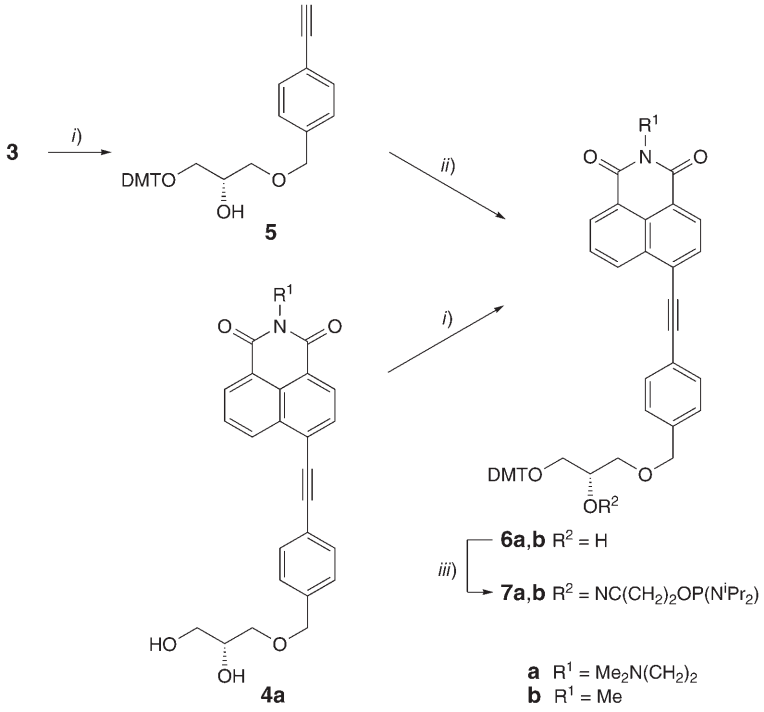

i) Dimethoxytrityl chloride (DMTCl), pyridine, 20°; **6a**: 60%, **5**: 73%. *ii)* **2b**, $Pd(PPh_3)_4$, CuI, Et_3N, DMF, 20°; **6b**: 65%. *iii)* $NC(CH_2)_2OP(N^iPr_2)_2$, diisopropylammonium tetrazolide, CH_2Cl_2, 0–20°; **7a**: 64%, **7b**: 89%.

Table 1. *Calculated and Found Masses of Synthesized Oligonucleotides*

No.	Sequence	*m/z* [Da]	
		calc.	found[a])
ON4	5′-CCCCTT**Y**TCTTTTTT-3′	4655.2	4654.1
ON7	5′-**Y**CCCCTTTCTTTTTT-3′	4655.2	4658.1
ON13	5′-CTCAAG**Y**CAAGCT-3′	4147.9	4147.8
ON16	5′-**Y**CTCAAGCAAGCT-3′	4147.9	4147.3
ON5	5′-CCCCTT**Z**TCTTTTTT-3′	4597.3	4596.8
ON8	5′-**Z**CCCCTTTCTTTTTT-3′	4597.3	4597.9
ON14	5′-CTCAAG**Z**CAAGCT-3′	4089.9	4089.8
ON17	5′-**Z**CTCAAGCAAGCT-3′	4089.9	4091.4

[a]) Determined by MALDI-TOF-MS.

tides containing an intercalator in the middle of the sequence were constructed to intercalate as a bulge without any opposite nucleobase.

The thermal stability of triplexes with the synthesized oligonucleotides towards the complementary duplex, **D1**, was assessed at two different pH values. The main difference between the T_m values at pH 6.0 and 7.2 is based on the protonation of cytosine, because only the protonated cytosine is able to form *Hoogsteen* bonds. The cytosine bases are protonated at lower pH value, which results in higher T_m values at pH 6.0 compared to pH 7.2. The thermal stability of triplexes formed with the naphthalimide TFOs **ON4**, **ON5**, **ON7**, and **ON8** was compared with the unmodified TFO **ON1**, with pyrene TFOs **ON3** and **ON6**, and with the naphthalene TFO **ON2**.

All modified sequences showed high T_m values of the triplexes compared to the unmodified **ON1** at both pH values. At pH 6.0, the stability of the modified sequences with the intercalators **Y** and **Z** were also measured at a wavelength of λ 400 nm besides λ 260 nm due to overlapping duplex melting and triplex melting at the latter wavelength. Since it was not attempted to perform curve resolution of duplex and triplex melting curves at 260 nm, it is not a surprise that the triplex melting was slightly lower (up to 3.5° for **ON8**) when the melting was measured at 400 nm. Therefore, the values at λ 400 nm were considered more accurate (*Table 2*).

The triplex stabilities of **ON4/D1** ($T_m^{260\,nm} = 48.0°$; $T_m^{400\,nm} = 47.5°$) and **ON5/D1** ($T_m^{260\,nm} = 45.0°$; $T_m^{400\,nm} = 43.0°$) are considerably increased compared to the unmodified triplex **ON1/D1** ($T_m^{260\,nm} = 27.0°$). Stabilization in the range of $\Delta T_m = 18.0 - 21.0°$ shows that we were able to establish a novel intercalating system with excellent binding properties. The difference of the T_m values between naphthalene in **ON2**, and the two naphthalimide sequences **ON4** and **ON5** was in the range of $\Delta T_m = 8.0 - 12.5°$ in all triplex measurements. The increased T_m values for **ON4/ON5** can be explained by stabilization *via* the imide function. The increased π-surface leads to additional $\pi - \pi$ stacking. The comparison of the T_m values of the sequences with the pyrene intercalator **X** (**ON3**) and the simple naphthalimide intercalator **Z** (**ON5**) demonstrated a better stabilization by the bigger aromatic pyrene system, at both pH values ($\Delta T_m = 3.0 - 6.0°$).

Table 2. *Melting-Temperature* (T_m [°]) *Data for Third-Strand and Mismatch Third-Strand Melting, Taken from UV Melting Curves* (λ 260 nm)[a])

TFO Sequences	Triplex 3′-CTGCCCCTTTCTTTTTT 5′-GACGGGGAAAGAAAAAA (**D1**		Triplex mismatch[b]) 3′-CTGCCCCTT*A*CTTTTTT 5′-GACGGGGAA*T*GAAAAAA (**D2**)
	pH 6.0	pH 7.2	pH 6.0
ON1 5′-CCCCTTTCTTTTTT	27.0	< 5.0	< 5.0
ON2 5′-CCCCTT**W**TCTTTTTT	35.0	13.5	n.d.[c])
ON3 5′-CCCCTT**X**TCTTTTTT	46.0	28.0	27.0
ON4 5′-CCCCTT**Y**TCTTTTTT	48.0 (47.5)[d])	27.0	31.5
ON5 5′-CCCCTT**Z**TCTTTTTT	45.0 (43.0)	22.0	26.5
ON6 5′-**X**CCCCTTTCTTTTTT	44.5	20.5	22.5
ON7 5′-**Y**CCCCTTTCTTTTTT	46.5 (46.0)	21.0	26.0
ON8 5′-**Z**CCCCTTTCTTTTTT	47.5 (44.0)	21.0	22.0

[a]) c = 1.5 μM of **ON1**–**8** and 1.0 μM of each strand of dsDNA (**D1**/**D2**) in 20 mM sodium cacodylate, 100 mM NaCl, 10 mM $MgCl_2$, pH 6.0 and 7.2; duplex T_m = 58.5° (pH 6.0) and 57.0° (pH 7.2). [b]) Bases in italics are mismatched to TFOs. [c]) Not determined. [d]) T_m Values determined at 400 nm for sequences for **Y** and **Z** are given in parentheses in cases of overlapped triplex and duplex melting.

For the naphthalimide intercalator **Y** (**ON4**) with the *N*-[2-(dimethylamino)ethyl] group, the T_m value was higher in the triplex measurement compared to the intercalator **Z** (**ON5**). A difference of $\Delta T_m = 4.5°$ was determined at pH 6.0 and $\Delta T_m = 5.0°$ at pH 7.2, when the intercalator was incorporated in the middle of the pyrimidine strand. When added to the 5′-end, the difference between these modifications (*i.e.*, **ON7** and **ON8**) was much lower. At pH 6.0, a difference of $\Delta T_m = 2.0°$ was measured, while, at pH 7.2, the T_m values were the same. The higher stability of **ON4** compared with the similar sequences **ON5** can be explained by the protonated dimethylamino group which forms a H-bond and partially quenches a negative charge on the phosphate backbone in the pyrimidine strand of the duplex. Presumably, this led to a reduced electrostatic repulsion between phosphates in the duplex backbone besides the electrostatic attraction between the TFO and the duplex. At pH 6.0, sequence **ON3** with pyrene had a lower T_m value than **ON4** ($\Delta T_m = 1.5°$).

The sensitivity to mismatches was studied for parallel triplexes using the duplex **D2** in which a base pair A·T, neighboring the insertion of the intercalator in the middle of the sequences, was reversed compared to the matching *Hoogsteen*-binding duplex **D1** (*Table 2*). For the neighboring mismatch, ΔT_m dropped by 16.5–19.0° for the sequences **ON3**–**ON5**. This is a high sensitivity to mismatch when compared to the work of *Zhou et al.* who aimed at stabilizing triplex formation of mismatch sequences. 9-Amino-6-chloro-2-methoxyacridine was inserted in the middle of the TFOs as a bulged insertion, and the ΔT_m values were determined within 10° for mismatched *Hoogsteen* bindings [13]. When the intercalator was attached at the 5′-end of **ON6**–**ON8** for the same duplex target, the T_m values dropped for the triplex mismatch in the range of 20.0–22.0° compared to the perfectly matched sequences.

For application of TFOs in the antigene strategy, not only a high sensitivity to mismatched triplexes is crucial, but also a sensitivity that minimize the affinity to other

possible targets where TFOs can form parallel or antiparallel duplexes with DNA or RNA single strands. Therefore, thermal-stability studies of parallel *Hoogsteen*-type duplexes with the modified sequences **ON2** – **ON8** towards **ON9** were performed. The sequence **ON2** with intercalator **W** showed only a stabilization of $\Delta T_m = 3.0°$ at pH 6.0 compared to the unmodified sequence **ON1**, whereas all other sequences showed an increase of thermal stability in the range of $\Delta T_m = 10.0 - 17.0°$ when compared with the wild-type parallel duplex (*Table 3*). However, this increase in melting temperatures is lower than those observed for the corresponding triplexes, which, in all cases, had considerably higher T_m values than the corresponding parallel duplex.

Table 3. *Melting-Temperature* (T_m [°]) *Data for Parallel Duplex and Parallel Mismatch Duplex*[a]) *Melting, Taken from UV Melting Curves* (λ 260 nm)

TFO Sequences	Parallel duplex 5′-GACGGGGAAAGAAAAAA (**ON9**)		Parallel mismatch[b]) 5′-GACGGGGAA*T*GAAAAAA (**ON10**)
	pH 6.0	pH 7.2	pH 6.0
ON1 5′-CCCCTTTCTTTTTT	19.0	< 5.0	< 5.0
ON2 5′-CCCCTT**W**TCTTTTTT	22.0	n.d.[c])	n.d.
ON3 5′-CCCCTT**X**TCTTTTTT	33.5	n.d.	21.5
ON4 5′-CCCCTT**Y**TCTTTTTT	35.0	27.5	17.0
ON5 5′-CCCCTT**Z**TCTTTTTT	29.0	21.5	17.0
ON6 5′-**X**CCCCTTTCTTTTTT	36.0	n.d.	n.d.
ON7 5′-**Y**CCCCTTTCTTTTTT	33.5	n.d.	23.5
ON8 5′-**Z**CCCCTTTCTTTTTT	32.5	n.d.	20.0

[a]) c = 1.0 μM of each strand in 20 mM sodium cacodylate, 100 mM NaCl, 10 mM $MgCl_2$, pH 6.0 or pH 7.2. [b]) Bases in italic are mismatched to TFOs. [c]) Not determined.

The sensitivity to mismatches was routinely studied for parallel duplexes with bulged insertion of **Y** and **Z** in the middle and at the 5′-end of the sequence at pH 6.0. For these measurements, the unmodified **ON10** was chosen, which is one of the strands from the mismatching duplex **D2**. Also for parallel duplexes, high sensitivity to mismatches was observed (*Table 3*).

The antiparallel-duplex measurements were performed with the mixed purine/pyrimidine sequences containing intercalators **Y** and **Z** (*i.e.*, **ON13**, **ON14**, **ON16**, and **ON17**) towards the complementary ssDNA (*i.e.*, **ON18**) and ssRNA (*i.e.*, **ON19**) to study hybridization affinity in *Watson – Crick*-type duplexes (*Table 4*). **ON18** is a strand of a mixed purine/pyrimidine duplex segment, which is highly conserved in 148 HIV-1 sequences [14], with the potential of improved antisense properties of oligonucleotides comprising the intercalators **Y** and **Z**. The intercalators were incorporated in the middle of a sequence as a bulge or at the 5′-end. The T_m values towards **ON18** and **ON19** were compared with the unmodified sequence **ON11**, and with pyrene TFOs **ON12** and **ON15**. Compared to the unmodified duplexes, the 5′-end-modified sequences showed an increase of the T_m values, towards DNA, of 4.5 – 7.0° and, towards RNA, of 5.0 – 6.5°. This can be explained by the lid effect of modifications at the 5′-end, which is

Table 4. *Melting-Temperature* (T_m [°]) *Data for Antiparallel Duplex*[a]) *Melting, Taken from UV Melting Curves* (λ 260 nm)

	Sequences	DNA 5′-AGCTTGCTTGAG (**ON18**)	RNA 5′-AGCUUGCUUGAG (**ON19**)
ON11	3′-TCGAACGAACTC	47.5	40.5
ON12	3′-TCGAAC**X**GAACTC	39.5	30.5
ON13	3′-TCGAAC**Y**GAACTC	40.0	38.5
ON14	3′-TCGAAC**Z**GAACTC	37.0	33.5
ON15	3′-TCGAACGAACTC**X**	54.0	45.5
ON16	3′-TCGAACGAACTC**Y**	54.5	47.0
ON17	3′-TCGAACGAACTC**Z**	52.0	46.5

[a]) c = 1.0 μM of each ON in 140 mM NaCl, 10 mM sodium phosphate buffer, 1 mM EDTA, pH 7.0.

ascribed to stacking of an aromatic system to the adjacent nucleobase [6c]. Sequences with modifications inserted in the middle of the sequences showed a destabilization of 7.5 – 10.0° towards DNA for all sequences (*i.e.*, **ON12** – **ON14**). Towards RNA, a similar destabilization of 7.0 – 10.0° was observed for the modified sequences **ON12** and **ON14**, whereas **ON13** only destabilized the duplex with 2.0° when compared with the unmodified duplex. These results eliminate the potential of using the new intercalators in antisense oligonucleotides. Instead, the destabilization can be a desired discrimination against antiparallel *Watson – Crick*-type duplexes when oligonucleotides are used for triplex formation. The different melting-temperature discrimination of **ON13** with 7.5° towards DNA and 2.0° towards RNA may be explained by the protonated dimethylamino group which interacts differently with the backbone of the dsDNA (B-type helix) and the DNA/RNA hybrid (between A- and B-type helix) [15].

Molecular-Modeling Studies. The molecular-modeling studies were performed on truncated triplexes with four base triplets on both sides of the intercalator which is incorporated in the middle of the sequence (*i.e.*, **ON4** and **ON5**) and the complementary duplex **D1**. Representative low-energy structures were generated with the AMBER* force field [16] in MacroModel 9.1 and selected after examination with Xcluster from *Schrödinger*.

The modeling study of intercalator **Y** and **Z** (*Fig. 2*) shows that the positions of the intercalators are similar, and that the benzene and the naphthalimide moieties are adding to the triplex stability *via* $\pi - \pi$ interaction with the nucleobases of the TFO and the purine strand of the duplex, respectively. In addition, the benzene moieties of the intercalators are slightly twisted in comparison to the naphthalimide moiety which has been indicated to be essential for stabilizing the adjacent nucleobases of the TFO [6a]. However, it seems that no or only low stabilizing interactions between the naphthalimide moiety and the pyrimidine strand of the duplex is formed as well as between the C≡C bond and the surrounding nucleobases. The enhanced triplex stability observed for intercalator **Y** might, therefore, be caused by protonation of the dimethylamino group which forms an ionic interaction with the negatively charged phosphate backbone of the pyrimidine strand of the duplex (*Fig. 2*). This interaction is enhanced by a H-bond from the dimethylammonium ion oriented in the direction of

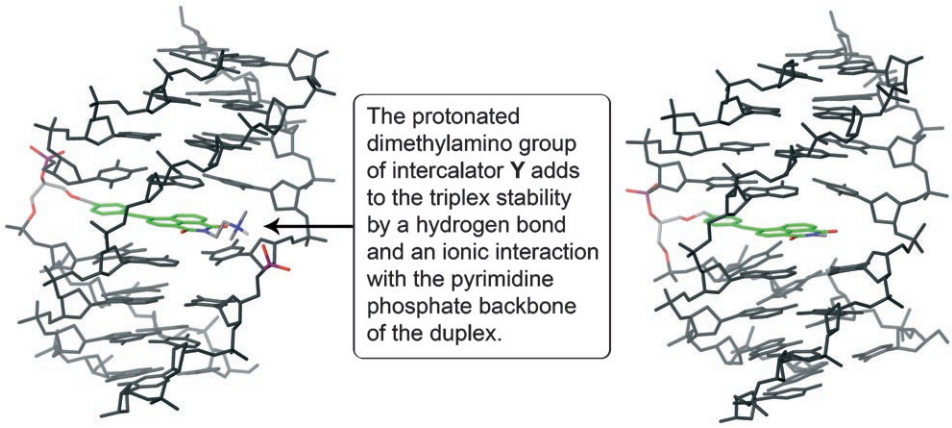

Fig. 2. *Modeling structure of protonated intercalator* **Y** (*left*) *and the neutral intercalator* **Z** (*right*)

the O-atom of the phosphate. It should be noted that the H-bonding takes place with the 3′-phosphate group of the neighboring thymine to the 3′-side in the pyrimidine strand of the duplex, and not to the phosphate group directly opposite to the intercalator. Even though this interaction seems to slightly distort the pyrimidine phosphate backbone of the duplex compared to intercalator **Z**, the molecular-modeling studies support the suggestion of an ionic interaction between the protonated dimethylamino group of intercalator **Y** with the phosphate backbone of the pyrimidine strand in the duplex, thereby adding to the stabilization of the triplex.

Molecular-modeling studies for the second conformation of the unsymmetrical intercalator where the naphthalimide is twisted by 180° around the C≡C bond were also performed. The position and interacting properties of the intercalator was almost identical to those shown in *Fig. 2*, and no optimal conformation could be assigned.

Conclusions. – The synthesis of the novel intercalators **Y** and **Z** *via Sonogashira* coupling, followed by phosphoramidite chemistry and incorporation into DNA sequences, showed a highly effective possibility of triplex stabilization. Naphthalimide intercalator **Z** in **ON5** with a Me group on the imide function showed a good triplex stability comparable to the corresponding pyrene intercalator. The naphthalimide intercalator **Y** in **ON4** with a side chain containing an amino function showed an even better stabilization of the triplex at two different pH values (6.0 and 7.2) compared to **Z**. The reason can be assigned to protonation of the amino group under physiological conditions, which reduces the electrostatic repulsion of the phosphates in the negatively charged backbone and forms a unique binding interaction to the duplex. TFOs containing **Y** are the first example of a stabilizing effect of an intercalator combined with an amino side chain that binds to the duplex backbone. This is supported by molecular-modeling studies which showed the ionic interaction of the protonated dimethylamino group of intercalator **Y** with the phosphate backbone of the duplex. In spite of the stabilizing effect of the intercalator, considerable destabilization of mismatch triplexes was detected by thermal-stability measurements. Therefore, a novel

possibility for the design of strongly binding TFOs with good discriminating properties between matched and mismatched triplexes was developed, and this may be useful in the antigene strategy. To avoid the complication of quadruplex formation of G-rich TFOs, we consider it possible to optimize the 7-deaza-2′-deoxyguanosine approach by using our compatible intercalator approach in a proper combination [17]. In this context, it could also be interesting to use 7-(aminoalkynyl)-7-deaza-2′-deoxyguanosine to take advantage of a possible ion-pair stabilization [18].

Experimental Part

General. Unmodified oligonucleotides were purchased from *DNA Technology A/S* (DK-Århus) and from *TAG Copenhagen A/S* (DK-Copenhagen). THF and toluene were dried over Na, and pyridine over KOH. DMF and MeCN were dried over 3-Å molecular sieves, and Et_3N and CH_2Cl_2 were dried over 4-Å molecular sieves. Solvents used for column chromatography (CC) were distilled prior to use. Petroleum ether (PE): b.p. 60–80°. Ar was used in the reactions involving inert atmosphere. The silica gel (0.040–0.063 mm) used for CC and anal. TLC analyses carried out on TLC plates *60 F_{254}* (*Merck*). M.p.: *Büchi* melting-point apparatus. NMR Spectra: *Varian Gemini-2000* spectrometer at 300 MHz for ^{1}H-, 75 MHz for ^{13}C-, and 121.5 MHz for ^{31}P-NMR; with Me_4Si as an internal standard for ^{1}H-NMR, deuterated solvents $CDCl_3$ (δ 77.16 ppm) and DMSO (δ 39.44 ppm) for ^{13}C-NMR, and 85% H_3PO_4 as an external standard for ^{31}P-NMR; δ in ppm, J in Hz. MS: *Ionspec 4.7 T HiResMALDI Ultima Fourier* transform (FT) mass spectrometer (*Ion Spec*, Irvine, CA). For accurate ion mass determination, the $[M+H]^+$ or $[M+Na]^+$ ion peak was matched using ions derived from the 2,5-dihydroxybenzoic acid matrix. Electrospray ionization (ESI)-MS: *4.7 T HiResESI Ultima* (FT) mass spectrometer; both spectrometers are controlled by the OMEGA data system. EI-MS: *Finnigan SSQ 710* instrument; in *m/z* (rel. %). MALDI-TOF-MS: of isolated oligonucleotides were determined on a *Voyager Elite* biospectrometry research station (*PerSeptive Biosystems*); in *m/z*.

1. *6-{[4-({[(2*R*)-2,3-Dihydroxypropyl]oxy}methyl)phenyl]ethynyl}-2-[2-(dimethylamino)ethyl]-1*H*-benzo[*de*]isoquinoline-1,3(2*H*)-dione*; **4a**). Diol **3** [6][9] (0.50 g, 2.42 mmol) was dissolved in anh. Et_3N (20 ml) and anh. DMF (20 ml), and flushed with Ar for 30 min. Then, *6-bromo-2-[2-(dimethylamino)ethyl]-1*H*-benzo[*de*]isoquinoline-1,3(2*H*)-dione* (**2a** [10]; 1.04 g, 3.00 mmol), $Pd(PPh_3)_4$ (0.127 g, 0.110 mmol), and CuI (0.023 g, 0.121 mmol) were added under a flow of Ar to the brown soln., and the soln. was stirred under Ar at 20°. After 20 h, the precipitate was filtered off, and CH_2Cl_2 (130 ml) was added to the orange soln., which was washed with 0.3M aq. soln. of EDTA ammonium salt (2 × 100 ml) and H_2O (3 × 70 ml). The org. layer was dried (Na_2SO_4), the solvent was evaporated under reduced pressure, and the residue was co-evaporated with toluene/EtOH 3:1 (2 × 30 ml). The residue was submitted to CC (CH_2Cl_2/MeOH 20:1) to afford **4a** (0.89 g, 78%). Yellow solid. M.p. 115–117°. ^{1}H-NMR ($CDCl_3$): 2.36 (*s*, Me_2N); 2.56 (br. *s*, CHO*H*); 2.66 (*t*, *J* = 6.9, $CH_2CH_2NMe_2$); 3.58–3.77 (*m*, $CH_2CH(OH)CH_2OCH_2$); 3.92–3.96 (*m*, C*H*OH); 4.30 (*t*, *J* = 7.1, $CH_2CH_2NMe_2$); 4.61 (*s*, $C_6H_4CH_2$); 7.38 (*d*, *J* = 8.1, 2 arom. H); 7.60 (*d*, *J* = 7.5, 2 arom. H); 7.79 (*t*, *J* = 7.8, 1 arom. H); 7.87 (*d*, *J* = 7.5, 1 arom. H); 8.50 (*d*, *J* = 7.5, 1 arom. H); 8.60 (*d*, *J* = 8.1, 1 arom. H); 8.64 (*d*, *J* = 8.4, 1 arom. H). ^{13}C-NMR ($CDCl_3$): 38.27 (NMe_2); 45.80 ($CH_2CH_2NMe_2$); 56.97 ($CH_2CH_2NMe_2$); 64.10 (CH_2OH); 70.83 (CHOH); 72.22 ($C_6H_4CH_2OCH_2$); 73.14 ($C_6H_4CH_2OCH_2$); 86.48 ($C{\equiv}C-C_6H_4$); 98.99 ($C{\equiv}C-C_6H_4$); 121.66, 122.99, 127.53, 127.67, 127.85, 128.15, 128.19, 130.53, 130.84, 131.65, 131.78, 132.13, 132.49, 139.59 (arom. C); 163.86, 164.13 (2 C=O). HR-MALDI-MS: 473.2073 ($[M+H]^+$, $C_{28}H_{29}N_2O_5^+$; calc. 473.2076).

2. *6-{[4-({[(2*R*)-2,3-Dihydroxypropyl]oxy}methyl)phenyl]ethynyl}-2-methyl-1*H*-benzo[*de*]isoquinoline-1,3(2*H*)-dione*; **4b**). Diol **3** ([6][9], 0.50 g, 2.42 mmol) was dissolved in anh. Et_3N (20 ml), and anh. DMF (20 ml), and flushed with Ar for 30 min. Then, *6-bromo-2-methyl-1*H*-benzo[*de*]isoquinoline-1,3(2*H*)-dione* (**2b** [11]; 0.87 g, 3.00 mmol), $Pd(PPh_3)_4$ (0.127 g, 0.121 mmol), and CuI (0.023 g, 0.121 mmol) were added under a flow of Ar to the brown soln., and the soln. was stirred under Ar at 20°. After 22 h, the precipitate was filtered off, CH_2Cl_2 (130 ml) was added to the orange mixture, which was washed with 0.3M aq. soln. of EDTA ammonium salt (2 × 100 ml) and with H_2O (3 × 70 ml). The org.

layer was dried (Na_2SO_4), the solvent was evaporated under reduced pressure, and the residue was co-evaporated with toluene/EtOH 3:1 (2 × 30 ml). The residue was submitted to CC (CH_2Cl_2/MeOH 20:1) to afford **4b** (0.31 g, 31%). Yellow solid. M.p. 164–166°. ^{1}H-NMR ((D$_6$)DMSO): 3.35 (*s*, MeN); 3.40–3.43 (*m*, $CH_2CH(OH)CH_2OCH_2$); 3.65–3.70 (*m*, C*H*OH); 4.53–4.57 (*m*, $CH_2CH(OH)CH_2OCH_2$); 4.58 (*s*, $C_6H_4CH_2$); 4.75 (br. *s*, CHO*H*); 7.47 (*d*, *J* = 8.1, 2 arom. H); 7.74 (*d*, *J* = 8.1, 2 arom. H); 7.91 (*t*, *J* = 8.1, 1 arom. H); 7.97 (*d*, *J* = 7.8, 1 arom. H); 8.35 (*d*, *J* = 7.5, 1 arom. H); 8.47 (*d*, *J* = 7.2, 1 arom. H); 8.66 (*d*, *J* = 7.5, 1 arom. H). ^{13}C-NMR ((D$_6$)DMSO): 26.58 (MeN); 63.00 (CH_2OH); 70.51 (CHOH); 71.64 ($C_6H_4CH_2OCH_2$); 72.15 ($C_6H_4CH_2OCH_2$); 85.86 ($C{\equiv}C-C_6H_4$); 98.58 ($C{\equiv}C-C_6H_4$); 120.10, 121.67, 122.40, 126.05, 127.02, 127.51, 128.02, 129.40, 129.68, 130.68, 130.93, 131.69, 140.67 (arom. C); 162.93, 163.23 (2 C=O). EI-MS: 415 (25, M^+). HR-MALDI-MS: 438.1296 ($[M+Na]^+$, $C_{25}H_{21}NNaO_5^+$; calc. 438.1317).

3. *6-({4-[({(2*S*)-3-[Bis(4-methoxyphenyl)(phenyl)methoxy]-2-hydroxypropyl}oxy)methyl]phenyl}-ethynyl)-2-[2-(dimethylamino)ethyl]-1*H*-benzo[*de*]isoquinoline-1,3(2*H*)-dione*; **6a**). Diol **4a** (0.67 g, 1.42 mmol) was dissolved in anh. CH_2Cl_2 (40 ml) and anh. Et_3N (0.22 ml, 1.56 mmol), and 4,4′-dimethoxytrityl chloride (DMTCl; 0.53 g, 1.56 mmol) was added under a flow of Ar. The soln. was stirred under Ar at 20°. After 17 h, an extra portion of DMTCl (0.12 g, 0.36 mmol) and Et_3N (0.05 ml, 0.36 mmol) was added, and, after another 7 h, another portion of DMTCl (0.05 g, 0.15 mmol) and Et_3N (0.02 ml, 0.14 mmol) was added. After a total reaction time of 45 h, H_2O (30 ml) was added, the two layers were separated, and the org. phase was washed with a sat. aq. soln. of $NaHCO_3$ (2 × 30 ml). The aq. phase was extracted with CH_2Cl_2 (25 ml). The combined org. layers were dried (Na_2SO_4), filtered, and evaporated under reduced pressure. The residue was co-evaporated with toluene/EtOH 1:1 (2 × 25 ml). The residue was submitted to CC (CH_2Cl_2/MeOH 1:1 with 0.5% Et_3N) to afford **6a** (0.657 g, 60%). Yellow foam. M.p. 82–83°. ^{1}H-NMR ($CDCl_3$): 2.37 (*s*, Me_2N); 2.46 (br. *s*, CHO*H*); 2.68 (*t*, *J* = 6.9, $CH_2CH_2NMe_2$); 3.23–3.26 (*m*, DMTOC*H*$_2$); 3.59–3.64 (*m*, $CH(OH)CH_2OCH_2$); 3.78 (*s*, 2 MeO); 3.97–4.03 (*m*, C*H*OH); 4.33 (*t*, *J* = 7.1, $CH_2CH_2NMe_2$); 4.58 (*s*, $C_6H_4CH_2$); 6.82 (*d*, *J* = 9.0, 4 H, DMT); 7.20–7.45 (*m*, 11 H, C_6H_4, DMT); 7.63 (*d*, *J* = 8.1, 2 arom. H); 7.83 (*t*, *J* = 7.9, 1 arom. H); 7.94 (*d*, *J* = 7.8, 1 arom. H); 8.55 (*d*, *J* = 7.5, 1 arom. H); 8.64 (*d*, *J* = 7.5, 1 arom. H); 8.72 (*d*, *J* = 8.4, 1 arom. H). ^{13}C-NMR ($CDCl_3$): 38.28 (Me_2N); 45.81 ($CH_2CH_2NMe_2$); 55.33 (MeO); 57.06 ($CH_2CH_2NMe_2$); 64.44 (CH_2ODMT); 70.09 (CHOH); 71.96 ($C_6H_4CH_2$); 72.93 ($C_6H_4CH_2OCH_2$); 86.24 (Ph_3C); 86.44 ($C{\equiv}C-C_6H_4$); 99.10 ($C{\equiv}C-C_6H_4$); 113.25, 121.53, 122.17, 123.06, 126.94, 127.19, 127.56, 127.78, 127.96, 128.25, 130.17, 130.56, 130.85, 131.79, 132.06, 132.54, 134.84, 136.08, 139.86, 144.92, 158.63 (arom. C); 163.92, 164.18 (2 C=O). HR-MALDI-MS: 775.3362 ($[M+H]^+$, $C_{49}H_{47}N_2O_7^+$; calc. 775.3383).

4. *(2*S*)-1-[Bis(4-methoxyphenyl)(phenyl)methoxy]-3-{[4-({2,3-dihydro-2-[2-(dimethylamino)ethyl]-1,3-dioxo-1*H*-benzo[*de*]isoquinolin-6-yl}ethynyl)benzyl]oxy}propan-2-yl 2-Cyanoethyl Di(propan-2-yl)-phosphoramidite*; **7a**). Alcohol **6a** (0.43 g, 0.56 mmol) was dissolved in anh. CH_2Cl_2 (45 ml) and flushed with Ar for 10 min, followed by addition of diisopropylammonium tetrazolide (0.12 g, 0.68 mmol). Then, 2-cyanoethyl tetraisopropylphosphordiamidite (0.08 g, 0.27 mmol) was added dropwise under external cooling with an ice-water bath and stirred under Ar at 20°. Extra addition of 2-cyanoethyl tetraisopropylphosphordiamidite (0.08 g, 0.27 mmol) was performed after 21, 40, and 46 h, resp. After 46 h, also *N*,*N*-diisopropylammonium tetrazolide (0.05 g, 0.29 mmol) was added. After 61 h, anal. TLC showed no more starting material, and the reaction was quenched with H_2O (30 ml). The layers were separated, and the org. phase was washed with H_2O (30 ml). The combined aq. layers were extracted with CH_2Cl_2 (25 ml). The combined org. layers were dried (Na_2SO_4), filtered, and silica gel (2.0 g) and pyridine (1.5 ml) were added, and solvents were removed under reduced pressure. The residue was purified by dry column vacuum chromatography (SiO_2; AcOEt/cyclohexane 0:10 → 5:5, with 0.5% Et_3N) to afford **7a** (0.35 g, 64%). Yellow oil. ^{31}P-NMR ($CDCl_3$): 150.34, 150.57.

5. *(2*S*)-1-[Bis(4-methoxyphenyl)(phenyl)methoxy]-3-[(4-ethynylbenzyl)oxy]propan-2-ol* (**5**). Diol **3** ([6][9], 0.23 g, 1.15 mmol) was dissolved in anh. pyridine (25 ml), and, under a flow of Ar, DMTCl (0.47 g, 1.40 mmol) was added, followed by stirring under Ar at 20°. After 36 h, the reaction was quenched with MeOH (1 ml), and the mixture was diluted with AcOEt (50 ml) and washed with a sat. aq. soln. of $NaHCO_3$ (2 × 30 ml). The H_2O phase was extracted with AcOEt (30 ml). The combined org. layers were dried (Na_2SO_4), filtered, and evaporated under reduced pressure. The residue was co-evaporated with toluene/EtOH 1:1 (2 × 25 ml), dissolved in anh. CH_2Cl_2 (20 ml) and anh. pyridine

(2 ml), and adsorbed on silica gel (1.2 g) by evaporation under reduced pressure. The residue was purified by dry column vacuum chromatography (SiO_2; AcOEt/cyclohexane 0:10 → 5:5, with 0.5% Et_3N) to afford **5** (0.43 g, 73%). Yellow foam. ^{1}H-NMR ($CDCl_3$): 2.40 (*d*, *J* = 4.8, CHO*H*); 3.06 (*s*, C≡CH); 3.20–3.23 (*m*, DMTOCH_2); 3.55–3.58 (*m*, CH(OH)CH_2OCH$_2$); 3.78 (*s*, 2 MeO); 3.97 (*m*, C*H*OH); 4.52 (*s*, $C_6H_4CH_2$); 6.81 (*d*, *J* = 9.0, 4 H, DMT); 7.20–7.50 (*m*, 13 H, arom. H, DMT). ^{13}C-NMR ($CDCl_3$): 55.34 (MeO); 64.43 (CH_2ODMT); 70.10 (CHOH); 71.81 ($C_6H_4CH_2$); 72.97 ($C_6H_4CH_2OCH_2$); 77.58 (C≡*C*−H); 83.63 (*C*≡C−H); 86.25 (Ph_3C); 113.26, 121.49, 127.53, 127.97, 128.26, 130.17, 132.30, 136.09, 139.05, 144.93, 158.64 (arom. C). HR-MALDI-MS: 531.2164 ([*M* + Na]$^+$, $C_{33}H_{32}NaO_5^+$; calc. 531.2147).

6. *6-({4-[({(2*S*)-3-[Bis(4-methoxyphenyl)(phenyl)methoxy]-2-hydroxypropyl}oxy)methyl]phenyl}-ethynyl)-2-methyl-1*H*-benzo[*de*]isoquinoline-1,3(2*H*)-dione*; **6b**). Compound **5** (0.40 g, 0.79 mmol) was dissolved in anh. Et_3N (10 ml) and anh. DMF (10 ml), and flushed with Ar for 30 min. Then, **2b** ([11], 0.29 g, 1.00 mmol), $Pd(PPh_3)_4$ (0.041 g, 0.035 mmol), and CuI (0.008 g, 0.042 mmol) were added under a flow of Ar to the soln., and the soln. was stirred under Ar at 20°. After 28 h, an extra portion of $Pd(PPh_3)_4$ (0.041 g, 0.035 mmol) and CuI (0.008 g, 0.042 mmol) were added, and, after a total reaction time of 40 h, CH_2Cl_2 (75 ml) and Et_3N (1 ml) were added to the mixture. The mixture was washed with 0.3M aq. soln. of EDTA ammonium salt (2 × 50 ml) and with H_2O (3 × 70 ml), followed by extraction of the combined aq. layers with CH_2Cl_2 (40 ml). The org. layer was dried (Na_2SO_4), evaporated under reduced pressure, and the residue was co-evaporated with toluene/EtOH 3:1 containing 0.5% Et_3N (2 × 40 ml). The crude material was dissolved in CH_2Cl_2 (20 ml) and pyridine (1.0 ml), and silica gel (1.6 g) was added, and the solvents were removed under reduced pressure. The residue, adsorbed on silica gel, was purified by dry column vacuum chromatography (SiO_2; AcOEt/cyclohexane 0:10 → 5:5 containing 0.5% Et_3N) to afford **6b** (0.38 g, 65%). Yellow foam. M.p. 84–86°. ^{1}H-NMR ($CDCl_3$): 2.47 (*d*, *J* = 5.1, CHO*H*); 3.21–3.26 (*m*, DMTOCH_2); 3.56 (*s*, MeN); 3.58–3.63 (*m*, CH_2CH(OH)CH_2OCH$_2$); 3.77 (*s*, 2 MeO); 3.97–4.13 (*m*, C*H*OH); 4.58 (*s*, $C_6H_4CH_2$); 6.82 (*d*, *J* = 9.0, 4 H, DMT); 7.20–7.45 (*m*, 11 H, C_6H_4, DMT); 7.65 (*d*, *J* = 8.1, 2 arom. H); 7.82 (*t*, *J* = 7.8, 1 arom. H); 7.93 (*d*, *J* = 7.5, 1 arom. H); 8.55 (*d*, *J* = 7.5, 1 arom. H); 8.64 (*d*, *J* = 7.2, 1 arom. H); 8.72 (*d*, *J* = 7.5, 1 arom. H). ^{13}C-NMR ($CDCl_3$): 27.19 (MeN); 55.33, (MeO); 64.44 (CH_2OH); 70.12 (CHOH); 71.96 ($C_6H_4CH_2OCH_2$); 72.94 ($C_6H_4CH_2OCH_2$); 86.27 (Ph_3C); 86.43 (*C*≡C−C_6H_4); 99.12 (C≡*C*−C_6H_4); 113.25, 121.53, 122.09, 122.98, 126.95, 127.57, 127.78, 127.96, 128.25, 130.18, 130.51, 130.86, 131.73, 132.07, 132.55, 132.65, 136.07, 139.62, 139.86, 144.93 (arom. C); 164.13, 164.39 (2 C=O). HR-MALDI-MS: 740.2587 ([*M* + Na]$^+$), $C_{46}H_{39}NNaO_7^+$; calc. 740.2624).

7. *(2*S*)-1-[Bis(4-methoxyphenyl)(phenyl)methoxy]-3-({4-[(2,3-dihydro-2-methyl-1,3-dioxo-1*H*-benzo[de]isoquinolin-6-yl)ethynyl]benzyl}oxy)propan-2-yl 2-Cyanoethyl Di(propan-2-yl)phosphoramidite*; **7b**). Alcohol **6b** (0.30 g, 0.42 mmol) was dissolved in anh. CH_2Cl_2 (25 ml) and flushed with Ar for 10 min, followed by addition of *N*,*N*-diisopropylammonium tetrazolide (0.09 g, 0.49 mmol). Then, 2-cyanoethyl tetraisopropylphosphordiamidite (0.16 g, 0.54 mmol) was added dropwise under external cooling with an ice-water bath, and the soln. was stirred under Ar at 20°. An extra portion of 2-cyanoethyl tetraisopropylphosphordiamidite (0.06 g, 0.21 mmol) and *N*,*N*-diisopropylammonium tetrazolide (0.04 g, 0.21 mmol) were added after 21 h. After 44 h, anal. TLC showed no more starting material, and the reaction was quenched with H_2O (25 ml). The layers were separated, and the org. phase was washed with H_2O (25 ml). The combined aq. layers were extracted with CH_2Cl_2 (25 ml). The combined org. layers were dried (Na_2SO_4), filtered, and silica gel (1.0 g) and anh. pyridine (1.0 ml) were added, and solvents were removed under reduced pressure. The residue was purified by dry column vacuum chromatography (SiO_2; AcOEt/cyclohexane 0:10 → 3:7 containing 0.5% Et_3N) to afford **7b** (0.34 g, 89%). Yellow foam. ^{31}P-NMR ($CDCl_3$): 150.26, 150.49.

8. *Molecular Modeling.* The molecular modeling was performed with the program Maestro v7.5 from *Schrödinger*. All calculations were conducted with AMBER* force field [16] and the GB/SA water model [19]. The dynamics simulations were performed with stochastic dynamics [20], a SHAKE algorithm to constrain bonds to H-atoms [21], a time step of 1.5 fs, and simulation temp. of 300 K. Simulation for 0.5 ns with an equilibration time of 150 ps generated 250 structures, which were all minimized using the PRCG method with convergence threshold of 0.05 kJ/mol. The minimized structures were examined with Xcluster from *Schrödinger*, and representative low-energy structures were selected. The starting

structures were generated with Insight II v97.2 from *MSI*, followed by incorporation of the desired intercalator between the two neighboring bases.

9. *Synthesis of Oligonucleotides.* DMT-On oligodeoxynucleotides were synthesized in a 0.2-μmol scale on CPG supports using *Expedite Nucleic Acid Synthesis System* model *8909* (*Applied Biosystems*), using 4,5-dicyanoimidazole as an activator and a 0.075 mM soln. of the corresponding phosphoramidites **7a** and **7b** in anh. CH_2Cl_2. The syringe was attached to the CPG support, and the soln. was pressed through the support giving a coupling time of twice 20 min for **7a** and of 20 min for **7b**. Purification of 5′-DMT-on oligonucleotides was accomplished by a reverse-phase semiprep. HPLC on a *Waters Xterra MS* C_{18} column. DMT Groups were cleaved with 80% AcOH (100 μl) for 20 min. Afterwards, H_2O (100 μl) and 3M aq. AcONa (50 μl) were added, and oligonucleotides were precipitated from 99% EtOH (550 μl). The modified oligonucleotides were confirmed by MALDI-TOF-MS analysis on a *Voyager Elite* biospectrometry research station from *PerSeptive Biosystems.* The purity of the final TFOs was controlled by ion-exchange chromatography using a *LaChrom* system from *Merck Hitachi* on a *GenPak-Fax* column (*Waters*).

10. *Thermal Stability Studies of Duplexes and Triplexes.* Melting profiles were performed on a *Perkin-Elmer* UV/VIS spectrometer *Lambda 35* with a *PTP-6* thermostat and fitted with a *Perkin-Elmer* Templab 2.00 Software. The parallel triplexes were formed by mixing the two strands of the *Watson–Crick* duplex each at a concentration of 1.0 μM and the TFO at a concentration of 1.5 μM in the corresponding buffer soln. (pH 6.0 or 7.2). The soln. was heated to 80° for 5 min for removal of air bubbles and afterwards cooled to 5° for 30 min. The duplexes were formed by mixing the two strands, each at a concentration of 1.0 μM in the corresponding buffer soln., followed by heating to 80° for 5 min and then cooling to 5° for 30 min. The absorbance of triplexes and duplexes was measured at λ 260 nm from 5 to 80° with a heating rate of 1.0°/min. Experiments were also performed at λ 400 nm. Each measurement was performed twice. The melting temperatures (T_m, °) were determined as the average value of both maxima of the first derivative plots of the melting curves.

REFERENCES

[1] S. Obika, *Chem. Pharm. Bull.* **2004**, *52*, 1399.

[2] a) V. V. Soyfer, N. P. Potaman, 'Triple-Helical Nucleic Acids', Springer Verlag, 1995, p. 166; b) E. Schmitt, P. Muller, M. Paramavisam, V. V. Filichev, N. Bomholt, J. Schwarz-Finsterle, G. Hildenbrand, E. B. Pedersen, L. E. Xodo, M. Hausmann, 'Integrative Design of Selectively Colocalizing Oligonucleotide Probes', Poster at the International Workshop, Integrative Bioinformatics, 4th Annual Meeting, September 10–12, 2007, Ghent, Belgium, 2007.

[3] a) S. M. Gryaznov, J.-K. Chen, *J. Am. Chem. Soc.* **1994**, *116*, 3143; b) V. Tereshko, S. M. Gryaznov, M. Egli, *J. Am. Chem. Soc.* **1998**, *120*, 269; c) F. Ehrenmann, J.-J. Vasseur, F. Debart, *Nucleosides Nucleotides Nucleic Acids* **2001**, *20*, 797; d) T. Michel, F. Debart, F. Heitz, J.-J. Vasseur, *ChemBioChem* **2005**, *6*, 1254.

[4] a) B. Cuenoud, F. Casset, D. Hüsken, F. Natt, R. M. Wolf, K.-H. Altmann, P. Martin, H. E. Moser, *Angew. Chem., Int. Ed.* **1998**, *37*, 1288; b) J. Wengel, *Acc. Chem. Res.* **1999**, *32*, 301; c) B.-W. Sun, B. R. Babu, M. D. Sørensen, K. Zakrzewska, J. Wengel, J.-S. Sun, *Biochemistry* **2004**, *43*, 4160; d) J. Basye, J. O. Trent, D. Gao, S. W. Ebbinghaus, *Nucleic Acids Res.* **2001**, *29*, 4873; e) T. Carlomagno, M. J. J. Blommers, J. Meiler, B. Cuenoud, C. Griesinger, *J. Am. Chem. Soc.* **2001**, *123*, 7364.

[5] a) L. E. Xodo, G. Manzini, F. Quadrifoglio, G. A. van der Marcel, J. H. van Boom, *Nucleic Acids Res.* **1991**, *19*, 5625; b) S. Hildbrand, A. Blaser, S. P. Parel, C. J. Leumann, *J. Am. Chem. Soc.* **1997**, *119*, 5499; c) V. Roig, U. Asseline, *J. Am. Chem. Soc.* **2003**, *125*, 4416.

[6] a) V. V. Filichev, E. B. Pedersen, *J. Am. Chem. Soc.* **2005**, *127*, 14849; b) V. V. Filichev, H. Gaber, T. R. Olsen, P. T. Jørgensen, C. H. Jessen, E. B. Pedersen, *Eur. J. Org. Chem.* **2006**, *17*, 3960; c) R. X.-F. Ren, N. C. Chaudhuri, P. L. Paris, I. S. Rumney, E. T. Kool, *J. Am. Chem. Soc.* **1996**, *118*, 7671.

[7] U. B. Christensen, E. B. Pedersen, *Nucleic Acids Res.* **2002**, *30*, 4918; A. A.-H. Abdel-Rahman, O. M. Ali, E. B. Pedersen, *Tetrahedron* **2005**, *52*, 15311.

[8] B. C. Froehler, S. Wadwani, T. J. Terhorst, S. R. Gerrard, *Tetrahedron Lett.* **1992**, *33*, 5307.

[9] I. Géci, V. V. Filichev, E. B. Pedersen, *Bioconjugate Chem.* **2006**, *17*, 950.
[10] P. Yang, Q. Yang, X. Qian, *Tetrahedron* **2005**, *61*, 11895.
[11] J.-X. Yang, X.-L. Wang, X.-M. Wang, L.-H. Xu, *Dyes Pigm.* **2005**, *66*, 83.
[12] K. Sonogashira, Y. Tohda, N. Hagihara, *Tetrahedron Lett.* **1975**, *16*, 4467.
[13] B.-W. Zhou, E. Puga, J.-S. Sun, T. Garestier, C. Hélène, *J. Am. Chem. Soc.* **1995**, *117*, 10425.
[14] A. Mujeeb, S. M. Kerwin, G. L. Kenyon, T. L. James, *Biochemistry* **1993**, *32*, 13419.
[15] L. Stryer, J. L. Tymoczko, J. M. Berg, in 'Biochemistry', 5th. edn., W. H. Freeman and Company, 2001, p. 747 – 749.
[16] S. J. Weiner, P. A. Kollman, D. A. Case, U. C. Singh, C. Ghio, G. Alagona, S. Profeta Jr., P. Weiner, *J. Am. Chem. Soc.* **1984**, *106*, 765; S. J. Weiner, P. A. Kollman, D. T. Nguyen, D. A. Case, *J. Comput. Chem.* **1986**, *7*, 230.
[17] F. Seela, Y. Chen, C. Mittelbach, *Helv. Chim. Acta* **1998**, *81*, 570.
[18] H. Rosemeyer, N. Ramzaeva, E.-M. Becker, E. Feiling, F. Seela, *Bioconjugate Chem.* **2002**, *13*, 1274.
[19] W. C. Still, A. Tempczyk, R. C. Hawley, T. Hendrickson, *J. Am. Chem. Soc.* **1990**, *112*, 6127.
[20] W. F. Van Gunsteren, H. J. C. Berendsen, *Mol. Simul.* **1988**, *1*, 173.
[21] J.-P. Ryckaert, G. Ciccotti, H. J. C. Berendsen, *J. Comput. Phys.* **1977**, *23*, 327.

Received January 4, 2008